Title: Modelling the dynamics of *Pinus sylvestris* forests after a die-off event under climate change scenarios

Running title: *Pinus sylvestris* resilience after a die-off event

Jordi Margalef-Marrase,[1] Roberto Molowny-Horas,[1] Luciana Jaime,[1] Francisco Lloret[1,2]

[1]Centre de Recerca Ecològica i AplicacionsForestals (CREAF), Bellaterra, 08193, Spain

[2]Unitat d'Ecologia, Universitat Autònoma de Barcelona, Bellaterra, 08193, Spain

Corresponding autor: Jordi Margalef-Marrase

jmargalefmarrase@gmail.com

https://orcid.org/0000-0003-4369-9918

Abstract

In recent decades, die-off events in *Pinus sylvestris* populations have increased. The causes of these phenomena, which are usually related to local and regional extreme hot droughts, have been extensively investigated from a physiological viewpoint. However, the consequences of die-off process in terms of demography and vegetation dynamics have been less thoroughly addressed.

Here, we projected *P. sylvestris* plot dynamics after a die-off event, under climate change scenarios, considering also their early demographic stages (i.e., seedlings, saplings and ingrowth from the sapling to adult class), to assess the resilience of *P. sylvestris* populations after such events. We used Integral Projection Models (IPMs) to project future plot structure under current climate, and under RCP4.5 and RCP8.0 climate scenarios, using climatic suitability – extracted from Species Distribution Models – as a covariable in the estimations of vital rates over time. Field data feeding IPMs were obtained from two successive surveys, at the end of the die-off event (2013) and four years later (2017), undertaken on populations situated across the *P. sylvestris* range of distribution in Catalonia (NE Spain).

Plots affected by die-off experienced a loss of large trees, which causes that basal area, tree diameter and tree density will remain lower for decades relative to unaffected plots. After the event, this situation is partially counterbalanced in affected plots by a greater increase in basal area and seedling recruitment into tree stage, thus promoting resilience. However, resilience is delayed under the climate-change scenarios with warmer and drier conditions involving additional physiological stress, due to a reduced abundance of seedlings and a smaller plot basal area.

The study shows lagged effect of drought-induced die-off events on forest structure, also revealing stabilizing mechanisms, such as recruitment and tree growth release, which

39 enhance resilience. However, these mechanisms would be jeopardized by oncoming
40 regional warming.

1. Introduction

Forest die-off is currently occurring across most biomes, and the consequences of the phenomenon are causing great concern, particularly under climate change conditions (Allen et al., 2010; Greenwood et al., 2017; Williams et al., 2013; Allen, Breshears, & McDowell, 2015; Anderegg et al., 2015; Clark et al., 2016). Forest die-off often occurs concurrently with extreme climatic events –i.e., droughts (Senf, Buras, Zang, Rammig, & Seidl, 2020) and heatwaves (Margalef-Marrase, Pérez-Navarro, & Lloret, 2020)– associated with the increased climatic variability that accompanies climate change, although other agents, such as insects and pathogens, can also intervene (Jaime et al., 2021; Wong & Daniels, 2017). The environmental and physiological mechanisms that ultimately cause tree mortality have been extensively studied (Adams et al., 2017; N. McDowell et al., 2018; Nathan G. McDowell & Allen, 2015), revealing the importance of the interaction between hydraulic failure and carbon starvation, particularly in conifer species (Adams et al., 2017). However, our understanding of the recovery of structural and compositional forest characteristics following these die-off events remains limited (but see Martínez-Vilalta and Lloret 2016, Batllori et al. 2020). In particular, the contribution of juvenile stages to this recovery and their involvement in tree mortality and growth rates (Clark et al. 2016) have not yet been sufficiently addressed.

Studies that have analyzed resilience in terms of the recovery of tree populations and their resistance to climate-induced die-off have revealed the important role of historical climatic conditions. These historical conditions can be translated to the climatic niche of the species, obtained from Species Distribution Models (SDMs) (Lloret & Kitzberger, 2018; Margalef-Marrase et al., 2020). SDMs are statistical methodologies that provide the probability of species occurrence by relating species presence and absence with bioclimatic variables (Guisan & Thuiller, 2005). The output of the models, ranging

between 0 to 1, can be used as a climatic suitability index for the populations of the studied species, that is, reflecting the conditions that historically a given population have experienced in relation to the climatic space where the species inhabit. Population climatic suitability values close to 0 indicate that a population has been living close to the edge of its climatic space, whereas populations with climatic suitability close to 1 indicate that a population has been living close to the core of the species's climatic space. Climatic suitability has been used to explain forest die-off resistance facing extreme climatic events (Lloret & Kitzberger, 2018; Margalef-Marrase et al., 2020) or to compare the responses to extreme climate events in different co-occurring species (Pérez Navarro et al., 2018; Sapes, Serra-Diaz, & Lloret, 2017).

Forest die-off events can especially affect those populations living under barely suitable historical climatic conditions, i.e., located close to their edge bioclimatic niche (Camarero et al., 2021; Mellert et al., 2016; Sánchez-Salguero, Navarro-Cerrillo, Swetnam, & Zavala, 2012). However, due to local adaptions, these populations may also experience high resistance (sensu Lloret et al. 2011) to events reproducing the climatic limits of the species' niche, while populations growing under suitable historical conditions – i.e., located close to their core bioclimatic niche– can be more vulnerable to drought events (Margalef-Marrase et al., 2020). In turn, populations living under more suitable historical climatic conditions may exhibit greater recovery, thus providing more resilience ("engineering resilience", sensu Pimm 1984) to abiotic disturbances, particularly those associated with extreme climatic events (Redmond, Weisberg, Cobb, & Clifford, 2018). This resilience could be due to the capacity of dominant species to remain and recover stand structural features, through further growth of remaining trees (Camarero et al., 2018) and/or the recruitment of new individuals, which in turn can be favoured by the micro-local conditions arising from the die-off event (Suarez & Lloret, 2018).

Integral Projection Models (IPMs) are used to describe changes over time in a given population structured by a continuous individual variable (e.g., size) (Easterling, Ellner, & Dixon, 2000). Like other demographic models, IPMs provide estimates of the asymptotic population growth-rate, stable size distribution, reproductive values, sensitivities and elasticities of the vital rates (Metcalf, McMahon, Salguero-Gómez, & Jongejans, 2013). IPMs are built from regression models describing vital rates –growth, survival and reproduction – from individual state variables (usually size or age), and they also can include environmental covariates (e.g., climate, competition and nutrient availability) (Merow et al., 2014). The use of IPMs in a forest population's dynamics has advantages over traditional population matrix models. For instance, IPMs can calculate survival, growth and recruitment with a reduced amount of data (e.g., in small populations with less than 300 individuals). IPMs are also more appropriate when the size variable is continuous (Ramula, Rees, & Buckley, 2009). Consequently, these models are broadly used in studies of the demography of forest populations and their dynamics (Dauer & Jongejans, 2013; Ferrer-Cervantes et al., 2012; Molowny-Horas, Suarez, & Lloret, 2017). *Pinus sylvestris* L. (Scots pine) has a wide range of distribution and is one of the most widespread tree species in the world. It extends across many biomes with different climates, from populations placed in eastern Siberia to relatively dry and warm locations in the Mediterranean Basin (Durrant, De Rigo, & Caudullo, 2016). On the Iberian Peninsula, *P. sylvestris* populations are located in the southern limit of its range of distribution (Matías & Jump, 2012), where the climatic conditions are less suitable for this species. These populations can therefore be more prone to die-off under climate change scenarios (Sánchez-Salguero et al., 2012), especially when facing recurrent and severe drought events (Vilà-Cabrera, Martínez-Vilalta, Galiano, & Retana, 2013). During 2005 and 2006, the Iberian Peninsula experienced a major drought followed by a period

of dry years (Banqué Casanovas et al. 2013; Füssel et al. 2017, see Appendix A, Fig.A1) that led to an acute drought event in 2012 (Camarero et al., 2018). As a consequence, forest die-off appeared across many woodland areas on the Iberian Peninsula, including Catalonia (Banqué Casanovas et al., 2013; Carnicer et al., 2011). More specifically, *P. sylvestris* populations experienced growth reduction (Camarero et al., 2018), loss of green canopy (Galiano, Martínez-Vilalta, & Lloret, 2010) and bark beetle infestations (Jaime et al., 2019) that eventually induced tree mortality, particularly in stands with high density (Galiano et al., 2010).

To sum up, during the next years disturbances across temperate forests related to climatic extreme events will likely be more frequent due to the impact of climate change. *P. sylvestris*, a common species in Europe and Iberian Peninsula is expected to suffer recurrent drought-induced die-off episodes, especially in its rear-edge populations. Thus, the resilience of this species facing an extreme climatic event can be diminished by a reduction of the climatic suitability in its range area. Therefore, the study of the forest dynamics following a drought induced die-off will be relevant to study population's resilience in a climate change context.

Here, we built an IPM to explore the dynamics of forests dominated by *P. sylvestris* following a drought-induced mortality event. Our main goal was to project the stand structure at mid-term (56 years after the drought-induced mortality event, in 2069) under different climatic change scenarios. We specifically considered the role of the recruitment stages and included the historical climatic suitability of each site as a covariate. We particularly addressed the following questions:

1) How do forest die-off events affect key vital rates that determine stand dynamics, such as recruitment, growth and mortality? Are these effects on key rates constant over time or, alternatively, are they exacerbated or depleted after the event? Do temporal trends of

recruitment, growth and mortality differ from one climatic scenario to another?

We hypothesise that drought-induced forest die-off will modify demographic trends such as growth and seedlings establishment after the following years of the event. Thus, we expect that climatic conditions, summarized by climatic suitability, are related to demographic trends. Nevertheless, the effect of die-off on demographic trends, will decrease over time due, among other reasons, the expansion over time of both canopy closure and competition. Therefore, we hypothesise that the effect of climate change on demographic trends will shift along the years following the die-off event.

2) Are the stands affected by die-off able to recover the same structure at mid-term (i.e., in 2069) as unaffected stands? Is this recovery different under distinct climate change scenarios? In other words, are the affected stands resilient, and does this resilience vary under different future climatic scenarios?

We hypothesise that recovery will be higher in stands at locations with more suitable climate. Under constant climate (no climate change scenario) we expect that stands with die-off will reach previous forest structure at mid-term (i.e. stands will be resilient). However, climate change can push previous suitable climatic conditions to harsher ones, reducing the recovery capacity of the stands affected by die-off, and delaying the time needed for the full stand recovery.

2. Methods

2.1. Study system

We performed the study in pure and mixed populations of *P. sylvestris* in Catalonia, North East of the Iberian Peninsula, in locations that had recently experienced drought-induced

164 forest die-off and tree mortality due to two drought events in 2005 and 2012, concurrent
165 with bark beetle infestation (Serra-Maluquer et al. 2018, Jaime et al. 2019, Appendix A,
166 Fig. A1). We selected 20 populations representing the whole climatic gradient across the
167 *P. sylvestris* range in Catalonia (Fig. 1). This selection was established by field visual
168 observation during late 2013 and early 2014. Due to the varying orography, these
169 populations experience different climate conditions, from suitable wet and cold
170 conditions (in the Pyrenees) to unsuitable drier and warmer conditions (in the Catalan
171 Coastal Range). The elevation of the studied sites ranges from 600 to 1,600m a.s.l., the
172 mean annual temperature ranges from 6.5 to 13°C and the annual precipitation from 600
173 to 1,100 mm per year (Karger et al. 2017, Fig. 1).

174 During 2013, two circular plots of 10m. diameter (314m^2) were established in each of the
175 20 selected populations. Then, we considered paired plots in each population: one plot
176 was set up in a stand affected by die-off and the other in an unaffected stand (located
177 close to each other, at a distance of about 50 to 150m). In affected plots, the loss of basal
178 area ranged from 30% to 90%, considering all the species of the plot (Appendix A Table
179 A1). The loss of basal area was estimated from all the dead trees identified in 2013. We
180 measured the size (diameter at breast height, dbh), distance and azimuth from the plot's
181 centre of both living and dead adult trees (dbh> 2.5cm). We also recorded all the *P.*
182 *sylvestris* recruits –dbh< 2.5cm– and classified them in two stages: (i) individuals up to
183 1.30m high and (ii) individuals taller than 1.30m. Finally, we recorded the following
184 stand characteristics: slope, aspect, total understorey cover, tree density (tree ha^{-1}) and
185 basal area ($m^2 \cdot ha^{-1}$). During 2017 (4 years after the first survey), we re-sampled the same
186 plots following the same protocol to record *P. sylvestris* tree mortality, individual
187 diametric growth, transitions between recruitment stages and ingrowth to the adult stage

188 from the recruiting ones. A total of 983 living trees were measured across the 20
189 populations.

190

191 **2.2. Climatic suitability modelling**

192 We used Species Distribution Models (SDMs) to obtain the historical climatic suitability
193 of the studied populations. *Pinus sylvestris* occurrences in the Iberian Peninsula (N =
194 10,383) were extracted from the EU-Forest dataset (Mauri, Strona, & San-Miguel-Ayanz,
195 2017). The EU-Forest occurrences dataset is based on almost 250,000 plots from the
196 National Forest Inventories of most European countries. Therefore, we did not use our
197 studied plots data to build the SDM. The use of data based on Forest Inventories allowed
198 us to include absence data in our model. We did not consider the occurrences of the
199 southernmost populations on the Iberian Peninsula, situated in the Sierra Nevada, as these
200 are usually considered a different infraspecific taxa (*P. sylvestris* var. *nevadensis*)
201 (Olmedo-Cobo, Gómez-Zotano, & Serrano-Montes, 2017) that could present differences
202 in niche characteristics due to local adaptations (Guisan, Thuiller, & Zimmermann, 2017).

203 We obtained SDM bioclimatic predictors from the CHELSA database version 2 (Fick &
204 Hijmans, 2017) with a spatial resolution of 30'' (~0.7km^2 at 40ºN), based on climatic
205 data from the 1979-2013 period. To calibrate the model, we used the mean of the six least
206 correlated bioclimatic variables in all the occurrences and absences of Iberian Scots pine
207 (isothermality, temperature seasonality, mean temperature of wettest quarter, mean
208 temperature of driest quarter, precipitation seasonality and precipitation of wettest
209 quarter), after testing the collinearity between nineteen bioclimatic variables by means of
210 the Variation Inflation Factor (VIF) (Marquaridt 1970).

211 The SDM algorithm used to calculate historical climatic suitability was Boosted
212 Regression Tree (BRT), applying the "Gbm R package" 2.1.3 (Ridgeway, 2007). We built
213 the species distribution model following the criteria used in the literature (Barbet-Massin,
214 Jiguet, Albert, & Thuiller, 2012; Elith, Leathwick, & Hastie, 2008; Pérez Navarro et al.,
215 2018). The calibration of the model was repeated three times, using k-fold cross-
216 validation with three different training and test datasets. The final model output was based
217 on all the occurrences. Model evaluation was based on the area under curve (AUC;
218 Hanley and McNeil 1982) and the variance explained as R squared coefficient (AUC =
219 0.9; r^2 = 0.72). These calculations were performed with the "caret R package" (Kuhn &
220 others, 2008). Then, we extrapolated our SDM for each studied plot, considering the
221 current climate reference data (1979-2013) in order to build up a control climate scenario.

222 For the calculations of future climatic suitability in our studied plots, we extrapolated the
223 SDM to both 2049 and 2069 (Appendix A, Figs. A2 and A3), which correspond,
224 respectively, to the average values of bioclimatic variables of the 2041-2060 and 2061-
225 2080 periods obtained from climatic scenarios based on future Representative
226 Concentration Pathways (RCP): RCP 4.5 and RCP 8.0, used in the Intergovernmental
227 Panel on Climate Change (IPCC) scenarios. For such purpose we used the average of 8
228 climate projections based on different atmospheric models (ACESS, CESM-BGR,
229 CESM-CAM5, CMCC-CM, FIO-ESM, IPSL-CM5A-MR, MIROC-5 and MPI-ESM-
230 MR) following the criteria of the literature (Sanderson, Knutti, & Caldwell, 2015). These
231 bioclimatic variables were also provided by the CHELSA climate database (Fick &
232 Hijmans, 2017). To make the change in climatic suitability progressive and not steeper,
233 we interpolated climate suitability for each year from 2017 to 2049 and from 2049 to
234 2069.

235 A reduction of climatic suitability under these two scenarios is expected to occur in our
236 plots (Appendix A, Figs. A2, A3, A6 and Table A2), but an increase of suitability could
237 also be possible in some regions (Appendix A, Fig. A3). RCP4.5 and RCP8.0 climate
238 scenarios are expected to be warmer and drier than current climate (Appendix B, Fig. B4
239 and Fig. B5). Particularly, RCP8.0 scenario is expected to be less suitable for *P. sylvestris*
240 than the RCP 4.5 scenario (Appendix B, Figs.B3, B4 and B5).
241

242 **2.3. Integral projection modelling**

243 We used IPMs as a tool to simulate population dynamics and to project future forest
244 structure. In this study, we have assumed that the tree vital rates depend on dbh at t_0. Vital
245 rates also depend on a set of environmental covariates (i.e., competition and climatic
246 suitability) through different analytical expressions (see below and accompanying
247 Appendix B). The input and output of a single run of an IPM consist of the continuous
248 distribution of the number of trees at times t and $t+\Delta$, where $\Delta= 4$ years in the present
249 work. Vital rates operate on the continuous input distribution of the number of trees per
250 size (dbh in our study), $N(dbh, t)$, through an integral equation, to yield the continuous
251 output distribution $N(dbh, t+\Delta)$. Due to its complexity, the integrals in the IPM
252 methodology are usually solved by means of numerical quadratures.The resulting
253 distribution $N(dbh, t+\Delta)$ can then be used to calculate structural variables such as tree
254 density, basal area and mean diameter. We describe in the Appendix B, and below, the
255 different vital rates regression used to build the final IPM.
256

257 **Survival**

258 Survival is described as the probability of a given adult tree to survive at time $t+\Delta$ as a
259 function of tree size and other environmental and plot-related variables (Coulson, 2012).

We could not calculate this probability directly from our plots since we did not find enough cases of mortality between the two censuses (2013 and 2017). Thus, we used the Third Spanish National Forest Inventory (IFN) data (DGCN, 2007) to build our survival function. We selected the inventory plots located in the Catalonian region that did not have management practices during the last decades. We assumed that the studied plots are representative of *P. sylvestris* forests in the region, and thus the determinants of mortality extracted from Catalonian IFN data correspond overall to those operating in the studied plots. We applied a generalized linear model with a binomial error structure to explain survival tree probability. Plot basal area, as well as both individual size at time 0 (dbh_{t0}) and $(dbh_{t0})^2$ were used as mortality predictors (Table 1). We did not include climatic suitability in this model since we found that, in the studied period, it has no effect on *P. sylvestris* survival probability in IFN plots. The rationale of this is that mortality events should be more related to climatic extremes (Neumann, Mues, Moreno, Hasenauer, & Seidl, 2017) than to climatic trends (Bottero et al., 2017) These mortality events can be more intense in denser populations-. Further, previous studies on *P. sylvestris* mortality using IFN data have shown that baseline mortality (in the absence of extreme drought events or other disturbances) is mainly related to stand competition and not to climate conditions (Ruiz-Benito, Lines, Gómez-Aparicio, Zavala, & Coomes, 2013). In our case, the inclusion of plot basal area in the survival function sought to consider these competition effects in the model. Furthermore, we assumed that our simulations could be conservative since future extreme climatic events have not been considered. Also, lagged mortality effects due to acute drought (Bigler, Gavin, Gunning, & Veblen, 2007; Klockow, Vogel, Edgar, & Moore, 2018) were not captured, i.e., the same survival rate after the drought event was applied to paired affected and unaffected plots. Moreover, mortality following the event could have been underestimated since we

285 only have data for 4 years after 2013 (i.e., 2017), and later drought-induced mortality may
286 have occurred after such a short time interval.

287

288 **Growth**

289 Tree growth is defined as the increment in size ($dbh_{t1} - dbh_{t0}$) during a given time interval
290 (in our case, 4 years). We calculated a growth function using Generalized Additive
291 Models for Location, Scale and Shape (GAMLSS, Rigby & Stasinopoulos, 2005) using
292 the "gamlss R package" (Stasinopoulos & Rigby, 2007). We estimated mu coefficient
293 (scale, mean) as a function of basal area (BA), tree plot density (N), climatic suitability
294 (CS), individual size (dbh_{t0}) and die-off effect (yes or no). Sigma coefficient (scale, e.g.,
295 variance) was estimated from basal area and dbh at t_0 (Table1, and text of Appendix B).

296 **Recruitment/Ingrowth**

297 Ingrowth is defined as the increment in the number of new adult trees during a given time
298 interval (in our case, 4 years), i.e., the number of saplings that become adults. Since the
299 seedlings and saplings of perennial plants often have different requirements and vital rates
300 than adult trees (Bertrand, Gégout, & Bontemps, 2011), we discretised different
301 recruitment classes: seedlings, saplings and ingrowth trees (small adults, ingrowth
302 hereafter). Because we had data on the total amount of seedlings, saplings and ingrowth
303 trees in each plot, we could compute a regression for the total number of individuals in
304 each of these three discrete recruitment stages using environmental covariates (basal area
305 and climatic suitability), the previous number of recruits in each discrete stage (expressed
306 as $n1_{t0}$ for the number of seedlings, and $n2_{t0}$ for the number of saplings) and die-off effect
307 (Table 2). We assume that the number of seedlings ($n1_{t1}$) does not depend on the size of
308 the adult trees in the plot. Since plots without recruitment stages were common, we built

309 the recruitment functions as zero-inflated regressions. We used the "psclR
310 package"(Jackman et al., 2020) to calculate these models. The size distribution of the
311 ingrowth was established from the ingrowth individuals data of the 2017 inventory
312 (Appendix B, Fig. B1f). For further information see text of Appendix B.

313

314 **Simulation**

315 Our IPM was built by combining calculated vital rates using numerical integration with
316 the Alternative Extended Simpson (Press, Flannery, Teukolsky, & Vetterling, 1989)
317 numerical quadrature rule. IPM outputs were individual sizes in terms of dbh. The upper
318 and lower limit of adult individual size were established as 150cm and 2.5cm dbh,
319 respectively, and we fixed 1,000 abcissa points. As a result, then we used a value of
320 0.147cm as the interval between abcissa points in the numerical quadrature rule. We can
321 extract several plot characteristics from the IPM outputs, such as tree plot density, basal
322 area, mean plot diameter, plot seedling and sapling density and ingrowth density (defined
323 as density of saplings that became adult in each model step, i.e., in 4 years). We used four
324 years step since it is the time between the two successive inventories. Climatic suitability
325 was used as an environmental covariable to capture how future climate trends affect *P.*
326 *sylvestris* forest dynamics. Thus, we simulated the IPM using climatic suitability under
327 three different climate scenarios: current constant climate (1979-2013 reference period)
328 and climate change scenarios corresponding to RCP4.5, and RCP 8.0 projections, for both
329 types of plots– those affected by die-off and those unaffected –over 52years (2017-2069)
330 in 4-year steps. We simulated forest dynamics in a hypothetical absence of new die-off
331 events.

332

333 **Validation**

334 Validation of the IPM numerical projections was carried out by evaluating the ability of
335 the full IPM simulations to reproduce the dynamics of the *P. sylvestris* tree stands between
336 $t = 2013$ and $t = 2017$ as compared to an alternative, simpler IPM (hereafter,
337 "Constant" model) in which the different functions specifying tree growth, survival and
338 recruitment, as well as the dynamics of seedlings and saplings, did not depend on any
339 predictor and only had a constant term (see Appendix C for further details). In almost all
340 cases, the IPM-projected model outperformed the "Constant" model, showing higher
341 Pearson correlation values and lower RMSE and MAD. On the other hand, performance
342 indices for the Number of adult trees (Appendix C, Table C1) were better for the
343 "Constant" model. A detailed inspection of model results revealed that the IPM-
344 projection underestimated the total number of trees in some of the stands. However,
345 model performance for the other four stand characteristics consistently showed better
346 results for the IPM-projection than for the "Constant" model.. For further information of
347 the IPM validation see Appendix C.

348

349 **2.4. Statistical analyses**

350 First, we built different Generalized Mixed Models (GLMMs) to assess how die-off
351 events determined stand dynamics overtime after the event, considering different future
352 climatic scenarios. Each plot was used as a replicate. The models' response variables
353 were, respectively: (1) basal area, (2) seedling density and (3) ingrowth density (density
354 of trees that became adult at given model time step), (4) sapling density, (5) ingrowth,
355 and (6) mean diameter, all of them extracted from IPM projections. The models'
356 explanatory variables were: die-off effect (yes-no), climatic scenario (current, constant

climate, RCP4.5, RCP8.5) and time (years) after the die-off event. Plot was included as random effect. To consider whether die-off effect also induces changes of dynamics responses across time and climatic scenario, we included the interaction between die-off effect and time, and the interaction between die-off effect and climatic scenario.

Secondly, we also built a GLMM to assess the resilience capacity at mid-term (projections until the year 2069). For such purpose, here we used several IPM outputs for the 2069 year as response variables: (1) basal area, (2) tree density (N), (3) seedling density, (4) sapling density, (5) ingrowth and (6) mean diameter. We used climatic scenario and die-off effect and their interaction as explanatory variables. Accordingly, we tested whether, at the mid-term of the time period, the structure of plots affected by die-off will differ from unaffected ones and whether the climatic scenario will reduce resilience. A significant reduction in the response variables in plots affected by die-off would therefore indicate a loss of resilience.

3. Results

3.1. Integral Projection Modelling

We found that survival probability was negatively related to plot basal area and tree square diameter at time t_0, while it was positively related to the dbh at t_0 (Table 1). This suggests that big trees, with a likely lower growth rate, tend to be less prone to die, a tendency that is reversed in the biggest ones, which are more prone to die (negative effect of the square dbh_0). The negative effect of basal area denotes that competition had a negative effect on tree survival. Also, tree growth was negatively related to those variables associated with competition (basal area and tree density). Conversely, tree growth was positively related to climatic suitability and dbh (Table 1). Also, the

relationship between growth and the square of the dbh is negative, denoting that the biggest trees are likely to growth less too. As regards the recruitment stages, seedling, sapling and ingrowth densities were negatively related to stand basal area. In contrast, both seedling and sapling densities were positively associated with seedling density at t_0. Moreover, sapling and ingrowth densities were positively related to the number of saplings at time t_0, while seedling density was also positively influenced by climatic suitability (Table 2).

3.2. Forest structure and recruitment over time

During the projected period of 2017-2069, we found significant correspondences between the structural and demographic variables – basal area, seedling density, sapling density, ingrowth density, tree density, mean tree diameter – and die-off effect, climate scenario and time since the die-off event. More specifically, basal area, sapling density and mean diameter were positively related to time since the die-off event; in contrast, both seedling density, ingrowth density and tree density were negatively related to the year since the die-off event (Table 3, Fig. 2). Over time, plots affected by die-off presented a significantly smaller basal area, and less adult tree densities. Conversely, they showed greater ingrowth, seedling and sapling densities. These effects remained throughout the whole simulated period (Fig. 2). Projections under climate change scenarios (RCP4.5, RCP8.0) led to a reduction in basal area, adult and seedling densities, as well as an increase in ingrowth density, compared to the projections using constant climate.

Furthermore, significant interactions emerged in our GLMMs comparing climatic scenarios. There were positive interactions between die-off effect and time since the die-off event for basal area, seedling density, ingrowth density, mean diameter and tree

density (Table 3). A negative interaction between climate change scenario and die-off effect emerged in the model with seedling density as the response variable. There was no interaction between die-off effect and climate change scenario for the other structural variables. This indicated that temporal patterns of simulated future basal area, ingrowth density, mean diameter and tree density differed according to the effect of the die-off on the plot – showing a greater increase in these response variables in plots affected by die-off –independently of climate change scenario. Overall, at mid-term we observed a convergent pattern of plot basal area among the plots affected by die-off and those unaffected, since plots that experienced die-off showed a greater increase in basal area than unaffected plots (Fig. 2) over time. As regards the temporal dynamics of seedlings and ingrowth density, the decrease over time was greater in plots affected by die-off than in unaffected ones; there was thus also a convergent pattern in the density of both seedling and ingrowth stages between the plots affected by die-off and those unaffected (Fig. 2).The negative interaction between die-off effects and climate change scenario on seedling density showed that the positive effect of the die-off effect was negatively modulated by the warmer and drier climate change scenario. Climatic change scenarios (both RCP4.5 and RCP8.0) induced a reduction in seedling density, resulting in fewer differences between affected and unaffected plots when comparing climate change projections with constant, climate projections (Fig.2).

3.3. Projected forest structure at mid-term

At the end of our projections (2069, i.e., 56 years after the die-off event), basal area and mean tree diameter were still significantly lower in plots affected by die-off than in unaffected ones (Fig. 2, Table 4). Moreover, these affected plots had a higher number of seedlings, saplings and ingrowth densities, resulting overall in a higher density of young

trees. However, the 2013 die-off event did not cause significant changes in adult tree density (Table 4).

The GLMM also showed that, in addition to die-off, climate change scenarios influenced almost all the above-mentioned structural variables: basal area, seedling density, sapling density, ingrowth density and mean diameter (Table 4). Projections using warmer RCP4.5 and RCP8.0 climate scenarios resulted in significantly lower basal area than projections using the constant, current climate scenario (1979-2013). Seedling density was also lower in both warmer climate change scenarios than in projections using the current constant, reference climate. However, projections using warmer climate change scenarios showed higher densities of saplings and ingrowth rate than projections using current constant climate.

Overall plot tree density did not significantly differ between the affected and unaffected plots, or between climate scenarios. Significant negative interaction between die-off effects and climate scenario emerged for basal area, seedling density, sapling density and mean diameter models. This interaction corresponds to a greater basal area difference between affected and unaffected plots in both climate change scenarios (RCP4.5 and RCP8.0, with harsher climatic conditions than current climate) at 2069, in comparison to projections using constant, current climate. In contrast, this interaction shows how the positive effect of the die-off on densities of these stages – seedlings and saplings –was attenuated when these warmer climate scenarios were considered. Moreover, the recovery of the mean diameter in plots affected by die-off was significantly lower for climate change scenarios than for the current constant climate scenario of the mean diameter in plots affected by die-off was significantly lower for climate change scenarios than for the current constant climate scenario.

4. Discussion

Drought-induced die-off events produce changes in both forest structure and demographic dynamics that persist at mid-term, as supported by our *P. sylvestris* study case. After 52 years of simulations, plots that formerly exhibited heavy die-off still have distinct structural characteristics: less basal area, smaller mean tree size and higher density of young trees (seedlings, saplings and ingrowths). Climate change scenarios exacerbate or mitigate these trends. The overall result is that the resilience of these forests in terms of basal area is not fully attained, in our case at a temporal scale of around half-century, since this structural characteristic continues to present lower values in plots affected by heavy die-off than in unaffected ones.

As regards the temporal dynamics of recruitment, the 2013 die-off event will induce a positive effect on seedling density in both short- and mid-term scenarios (up to the year 2069). However, overall seedling density and ingrowth diminish overtime, as expected in forest succession, while the canopy gets closed (Oliver, Larson, & others, 1996). This decrease over time was lower in die-off plots, consistent with a positive effect on the recruitment of die-off due to gap opening. This effect would remain at mid-term, probably because canopy closure will remain at some extent open in plots affected by die-off, in agreement with their smaller basal area, than in unaffected plots. In the short term (first years of our simulation period), canopy openness in these disturbed plots is expected to promote an increase in both the establishment and survival of seedlings (Macek et al., 2017), especially in species such as *P. sylvestris*, which has a semi-intolerant shade character (Castro, Zamora, Hódar, & Gómez, 2004; Niinemets & Valladares, 2006). Moreover, the reduction in climatic suitability due to climate change (Appendix A, Figs. A1-A3) for this species during the years following the event will be translated into a decline in the number of seedlings, particularly in plots that experienced die-off (see

479 interaction between die-off effect and climate scenario, Table 3). In this way, the positive
480 effect on seedling abundance due to the canopy openness created by the die-off would be
481 attenuated by the decline in climatic suitability in the following years (up to 2069). Other
482 studies also highlight the capacity of *P. sylvestris* to establish themselves and compete in
483 forest gaps, although this is jeopardised in populations close to the species' climatic
484 tolerance limit (Galiano, et al., 2013; Vilà-Cabrera et al., 2013).

485 Basal area and tree density in affected and unaffected die-off plots will, in their turn,
486 hypothetically converge with time in our simulations, indicating that (i) in plots affected
487 by die-off, growth rates in surviving trees would be higher than in unaffected plots, (ii)
488 adult mortality would be lower in affected plots than in unaffected plots, and (iii) seedling
489 establishment and higher densities of younger trees would be higher in affected plots,
490 resulting in more net ingrowth. Overall, this greater increase in basal area in die-off plots
491 is probably enhanced by reduced competition for light, nutrients and water (Nambiar &
492 Sands, 1993). This is consistent with other studies which have found that less dense tree
493 populations should be more resistant to future droughts and heatwaves (Bottero et al.,
494 2017). Also, more growth resistance has been observed in managed or thinned stands
495 during perturbations driven by climatic change (Aldea et al., 2017). Our results suggest
496 that self-thinning induced by drought events could also lead to an increase in post-drought
497 growth -recovery- and, hypothetically, to induce stands to be more resistant to further
498 disturbances. These compensatory recovery -engineering resilience- mechanisms seem to
499 operate even at mid-term, as seen by the converging trends of the basal area in affected
500 and unaffected plots over time. This convergence would be promoted by the
501 establishment of new individuals (seedlings) during the years following the die-off event
502 and the consequent high ingrowth.

503 However, according to our projections, the differences in basal area between the two types
504 of plots would remain significant in 2069, even though the basal area in affected plots
505 would reach similar values in 2069 to those observed in unaffected plots in 2013. This is
506 due to the long time period needed to replace the large trees that died during the drought
507 event. This is reflected in lower tree density in the years after the drought, and in smaller
508 tree size (on average) throughout the entire period in affected plots. Overall, in the
509 absence of further disturbances, full resilience would occur beyond 2069 in our
510 simulations, when plots with previous die-off would eventually attain levels of basal area
511 similar to those of unaffected plots. We also observed that adult tree density in die-off
512 plots will reach the same values as unaffected plots by 2069, approximately.
513 Nevertheless, as noted above, this convergence does not correspond to a similar value of
514 total plot basal area. In plots with die-off effects, the ingrowth is higher, probably due to
515 the loss of competition and the increase in both seedling and sapling establishment and
516 survival; consequently, adult trees in die-off plots would generally be younger and thinner
517 than those in unaffected plots. This pattern of forest regeneration, with younger
518 individuals and high turnover rates, is consistently observed abroad when a regime of
519 forest disturbance is modified by extreme climatic events such as drought (McDowell et
520 al., 2020).

521 Nevertheless, our simulations did not consider future mortality induced by further
522 extreme droughts, and we assumed that mortality is driven by competition rather than by
523 climatic suitability. Mortality and die-off will be conditioned, however, by the emergence
524 of extreme climatic events such as droughts and heatwaves (Lloret & Kitzberger, 2018)
525 that could push back succession or even provoke the collapse of these forest communities
526 (Harris et al., 2018). Therefore, the emergence of new extreme climatic events, would

527 conditionate the recovery of the previously affected plots, although we expect less
528 severity in terms of die-off in stands previously affected.

529 At mid-term, scenarios of warmer climate would result in a reduction in basal area in
530 plots affected by die-off, probably due to reduced growth in *P. sylvestris* trees (Table 1).
531 Growth patterns of *P. sylvestris*, including growth recovery and resilience after drought,
532 are closely related to climatic conditions, particularly temperature and potential
533 evapotranspiration (PET) prior to and after the drought event (Hereş, Martínez-Vilalta, &
534 López, 2012). Thus, future warmer climates are expected to induce a decline in growth
535 and loss of resilience across the Catalonian region (Bose et al., 2020), as we also observed
536 in our results. The mechanisms involved in this predicted/expected reduction in resilience
537 include a partial or total hydraulic failure of trees (Adams et al., 2017), as well as a loss
538 of leaf area and depletion of carbon reserves (Galiano, Martínez-Vilalta, & Lloret, 2011),
539 which could eventually lead to delayed mortality (Jump et al., 2017).

540 Self-thinning induced by die-off could bring populations to a new situation with less basal
541 area and, therefore, with less intra-specific competition, which, in turn, would make them
542 hypothetically more resistant to future climatic events (Sohn, Hartig, Kohler, Huss, &
543 Bauhus, 2016). However, populations close to their climatic tolerance limit could be even
544 less resilient at mid-term, since the establishment of *P. sylvestris* seedlings could be less
545 effective than the recruitment of other co-existing species (Galiano et al., 2013; Vilà-
546 Cabrera et al., 2013). Concurrently, a continuous reduction in climatic suitability will
547 diminish this seedling establishment at mid-term, as seen in our results. Moreover, future
548 droughts and xeric conditions may cause seedling establishment to decline after
549 disturbances such as wildfires (Elvira et al., 2021) and windthrows (Csilléry et al., 2017),
550 thus increasing the risk of loss of resilience in these populations. Furthermore, ingrowth
551 will increase under warm future climate conditions (as expected in RCP4.5 and RCP8.0

552 scenarios), due to (i) niche differentiation in this age class, which may also experience
553 facilitation (Canham & Murphy, 2017), (ii) increased capacity of younger trees to survive
554 and grow in warmer conditions (Peltola et al. 2002, Margalef-Marrase, Bagaria, & Lloret,
555 2022) and (3) loss of intra-specific competition with gap openings (De Chantal, Leinonen,
556 Kuuluvainen, & Cescatti, 2003). However, this increase in new adults will not be
557 translated into a greater plot basal area, on the time scale considered, but would instead
558 lead to younger forests with thinner trees (McDowell et al. 2020).

559 Under climate change, dendrological studies suggest a growth decline at tree-level in the
560 rear-edge distribution of *P. sylvestris* populations, due to an increase in water deficit
561 (Camarero et al., 2021; Hereş et al., 2012). This tendency can eventually lead to tree
562 death. Nevertheless, few studies have addressed growth and resilience at plot level after
563 drought-induced die-off events by considering the response of the remaining trees.
564 Demographic models such IPMs are appropriate tools for assessing future tendencies in
565 the tree populations of forests (Molowny-Horas et al., 2017; Sánchez-Velásquez, Pineda-
566 López, Ibarra-Zavaleta, & López-Serrano, 2021). One key aspect of our research is the
567 coupling of seedling and sapling dynamics with growth and survival functions, as well as
568 the introduction of climatic suitability as a covariate. This integration allows us to capture
569 a continuous picture of changes in plot structure over the projected time period. Moreover,
570 the use of IPMs allows us to analyze the ways in which self-replacement is determined
571 by climate change and die-off events (Batllori et al., 2020), in contrast to dendrological
572 approaches that do not consider regeneration dynamics and thus underestimate resilience
573 at the population level. This study highlights the relevance of integrating the dynamics of
574 different age classes (Ettinger & HilleRisLambers, 2013), particularly the recruiting
575 stages, at plot level, where interacting mechanisms such as climate and competition could
576 operate distinctly in sites with different degrees of drought-induced effects.

Conclusions

There is increasing concern about forest mortality resulting from the intensification of the drivers behind die-off events, as expected in the near-future climate change scenario. Some studies have suggested a loss of forest growth and resilience after drought events (Bose et al., 2020) and a likelihood of vegetation shifts (Batllori et al., 2020), but the time that has passed since most of such events were recorded is insufficient to verify the mid- and long-term consequences. Although simulations do not predict the future, they do make it possible to analyze the ways in which current die-off events can influence future population dynamics. IPMs constitute a useful tool for this purpose, since they allow us to assess the relevance of the different processes that determine forests dynamics and structure.

Our results show that, despite the capacity of Catalonian *P. sylvestris* forests to recover their structure after drought-induced die-off events (largely due to the recruitment and growth of young trees), this recovery does not appear to be immediate (during the following 50 years after the die-off event). The effects of these events could linger for long periods (more than 50 years, up to 2069 in our study system), mostly due to a loss of large trees during the drought events, which can only be replaced by new trees several decades later. This reduced resilience would diminish even more under climate change scenarios that imply extreme episodes of high temperature and water stress.

Author Contributions Statement

F. Lloret, J. Margalef-Marrase and R. Molowny-Horas conceived the ideas and designed the methodology; L. Jaime and J. Margalef-Marrase collected field data; R. Molowny-Horas and J. Margalef-Marrase analyzed the data; J. Margalef-Marrase led the writing of

600 the manuscript. All authors contributed critically to the drafts and gave final approval for
601 publication.

602 **Acknowledgements**

603 We thank the CHELSA climate database for making their data freely available online.
604 This study was funded by the Spanish Ministry of Education through doctoral grant no.
605 FPU15/04593, by the Spanish Ministry of Economy and Competitiveness through the
606 projects BIOCLIM (CGL2015-67419-R) and RESIBIO (PID2020-115264RB-I00) and
607 by the AGAUR 2017 SGR 1001 grant (Generalitat de Catalunya). We acknowledge O.
608 Calvet for his help in the field work. We also thank ML. Suárez for the datation of the
609 dead trees. The authors have no affiliation with any organization with a direct or indirect
610 financial interest in the subject matter discussed in the manuscript.
611

612 **Data Availability Statement**

613 *P. sylvestris* occurrences data were extracted from the EU-Forest occurrence datasets that
614 are openly available at Mauri et al. (**2017**; **https://doi.org/10.1038/sdata.2016.123**).
615 Climatic time series are openly available in CHELSA at **http://chelsa-**
616 **climate.org/downloads**.
617 R-code and other datasets that support the findings of this study are available from the
618 corresponding author upon reasonable request.
619

620 **References**

621 Adams, H. D., Zeppel, M. J. B., Anderegg, W. R. L., Hartmann, H., Landhäusser, S. M., Tissue,
622 D. T., … McDowell, N. G. (2017). A multi-species synthesis of physiological mechanisms
623 in drought-induced tree mortality. *Nature Ecology and Evolution*, *1*(9), 1285–1291.
624 https://doi.org/10.1038/s41559-017-0248-x

625 Aldea, J., Bravo, F., Bravo-Oviedo, A., Ruiz-Peinado, R., Rodríguez, F., & del Río, M. (2017).
626 Thinning enhances the species-specific radial increment response to drought in
627 Mediterranean pine-oak stands. *Agricultural and Forest Meteorology*, *237–238*, 371–383.
628 https://doi.org/10.1016/j.agrformet.2017.02.009

629 Allen, C. D., Breshears, D. D., & McDowell, N. G. (2015). On underestimation of global
630 vulnerability to tree mortality and forest die-off from hotter drought in the Anthropocene.
631 *Ecosphere*, *6*(8), 1–55. https://doi.org/10.1890/ES15-00203.1

632 Anderegg, W. R. L., Hicke, J. A., Fisher, R. A., Allen, C. D., Aukema, J., Bentz, B., … Zeppel,
633 M. (2015). Tree mortality from drought, insects, and their interactions in a changing
634 climate. *New Phytologist*, *208*(3), 674–683. https://doi.org/10.1111/nph.13477

635 Banqué Casanovas, M., Vayreda Duran, J., & Martínez-Vilalta, J. (2013). Monitoreo del
636 decaimiento de los bosques de Cataluña: Proyecto DEBOSCAT. In Sociedad Española de
637 Ciencias Forestales (Ed.), *6º Congreso Forestal Español* (pp. 1–11). Gasteiz.

638 Barbet-Massin, M., Jiguet, F., Albert, C. H., & Thuiller, W. (2012). Selecting pseudo-absences
639 for species distribution models: How, where and how many? *Methods in Ecology and*
640 *Evolution*, *3*(2), 327–338. https://doi.org/10.1111/j.2041-210X.2011.00172.x

641 Batllori, E., Lloret, F., Aakala, T., Anderegg, W. R. L., Aynekulu, E., Bendixsen, D. P., …
642 Zeeman, B. (2020). Forest and woodland replacement patterns following drought-related
643 mortality. *Proceedings of the National Academy of Sciences*, *117*(47), 202002314.
644 https://doi.org/10.1073/pnas.2002314117

Bertrand, R., Gégout, J. C., & Bontemps, J. D. (2011). Niches of temperate tree species converge towards nutrient-richer conditions over ontogeny. *Oikos*, *120*(10), 1479–1488. https://doi.org/10.1111/j.1600-0706.2011.19582.x

Bigler, C., Gavin, D. G., Gunning, C., & Veblen, T. T. (2007). Drought induces lagged tree mortality in a subalpine forest in the Rocky Mountains. *Oikos*, *116*(12), 1983–1994. https://doi.org/10.1111/j.2007.0030-1299.16034.x

Bose, A. K., Gessler, A., Bolte, A., Bottero, A., Buras, A., Cailleret, M., … Rigling, A. (2020). Growth and resilience responses of Scots pine to extreme droughts across Europe depend on predrought growth conditions. *Global Change Biology*, *26*(8), 4521–4537. https://doi.org/10.1111/gcb.15153

Bottero, A., D'Amato, A. W., Palik, B. J., Bradford, J. B., Fraver, S., Battaglia, M. A., & Asherin, L. A. (2017). Density-dependent vulnerability of forest ecosystems to drought. *Journal of Applied Ecology*, *54*(6), 1605–1614. https://doi.org/10.1111/1365-2664.12847

Camarero, J. J., Gazol, A., Sangüesa-Barreda, G., Cantero, A., Sánchez-Salguero, R., Sánchez-Miranda, A., … Ibáñez, R. (2018). Forest growth responses to drought at short- and long-term scales in Spain: Squeezing the stress memory from tree rings. *Frontiers in Ecology and Evolution*, *6*(FEB), 1–11. https://doi.org/10.3389/fevo.2018.00009

Camarero, J. J., Gazol, A., Sangüesa-Barreda, G., Vergarechea, M., Alfaro-Sánchez, R., Cattaneo, N., & Vicente-Serrano, S. M. (2021). Tree growth is more limited by drought in rear-edge forests most of the times. *Forest Ecosystems*, *8*(1), 1–15. https://doi.org/10.1186/s40663-021-00303-1

Canham, C. D., & Murphy, L. (2017). The demography of tree species response to climate: Sapling and canopy tree survival. *Ecosphere*, *8*(2). https://doi.org/10.1002/ecs2.1701

Carnicer, J., Coll, M., Ninyerola, M., Pons, X., Sanchez, G., & Penuelas, J. (2011). Widespread crown condition decline, food web disruption, and amplified tree mortality with increased

climate change-type drought. *Proceedings of the National Academy of Sciences*, *108*(4), 1474–1478. https://doi.org/10.1073/pnas.1010070108

Castro, J., Zamora, R., Hódar, J. A., & Gómez, J. M. (2004). Seedling establishment of a boreal tree species (Pinus sylvestris) at its southernmost distribution limit: Consequences of being in a marginal Mediterranean habitat. *Journal of Ecology*, *92*(2), 266–277. https://doi.org/10.1111/j.0022-0477.2004.00870.x

Clark, J. S., Zimmermann, N. E., Schwartz, M. W., Matthews, S., Jackson, S. T., Allen, C. D., … Davis, F. W. (2016). The impacts of increasing drought on forest dynamics, structure, and biodiversity in the United States. *Global Change Biology*, *22*(7), 2329–2352. https://doi.org/10.1111/gcb.13160

Coulson, T. (2012). Integral projections models, their construction and use in posing hypotheses in ecology. *Oikos*, *121*(9), 1337–1350. https://doi.org/10.1111/j.1600-0706.2012.00035.x

Csilléry, K., Kunstler, G., Courbaud, B., Allard, D., Lassègues, P., Haslinger, K., & Gardiner, B. (2017). Coupled effects of wind-storms and drought on tree mortality across 115 forest stands from the Western Alps and the Jura mountains. *Global Change Biology*, *23*(12), 5092–5107. https://doi.org/10.1111/gcb.13773

Dauer, J. T., & Jongejans, E. (2013). Elucidating the Population Dynamics of Japanese Knotweed Using Integral Projection Models. *PLoS ONE*, *8*(9), 1–11. https://doi.org/10.1371/journal.pone.0075181

De Chantal, M., Leinonen, K., Kuuluvainen, T., & Cescatti, A. (2003). Early response of Pinus sylvestris and Picea abies seedlings to an experimental canopy gap in a boreal spruce forest. *Forest Ecology and Management*, *176*(1–3), 321–336. https://doi.org/10.1016/S0378-1127(02)00273-6

DGCN. (2007). Tercer Inventario Forestal Nacional. *Direcci*[illegible]*n General De Conservaci*[illegible]*n De La Naturaleza, Ministerio De Medio Ambiente*.

695 Durrant, T. H., De Rigo, D., & Caudullo, G. (2016). Pinus sylvestris in Europe: distribution,
696 habitat, usage and threats. *European Atlas of Forest Tree Species*, 132–133.

697 Easterling, M. R., Ellner, S. P., & Dixon, P. M. (2000). Size-specific sensitivity: applying a new
698 structured population model. *Ecology*, *81*(3), 694–708.

699 Elith, J., Leathwick, J. R., & Hastie, T. (2008). A working guide to boosted regression trees.
700 *Journal of Animal Ecology*, *77*(4), 802–813. https://doi.org/10.1111/j.1365-
701 2656.2008.01390.x

702 Elvira, N. J., Lloret, F., Jaime, L., Margalef-Marrase, J., Navarro, M. Á. P., & Batllori, E.
703 (2021). Species climatic niche explains post-fire regeneration of Aleppo pine (Pinus
704 halepensis Mill.) under compounded effects of fire and drought in east Spain. *Science of*
705 *The Total Environment*, *798*, 149308.

706 Ettinger, A. K., & HilleRisLambers, J. (2013). Climate isn't everything: Competitive
707 interactions and variation by life stage will also affect range shifts in a warming world.
708 *American Journal of Botany*, *100*(7), 1344–1355. https://doi.org/10.3732/ajb.1200489

709 Ferrer-Cervantes, M. E., Méndez-González, M. E., Quintana-Ascencio, P. F., Dorantes, A.,
710 Dzib, G., & Durán, R. (2012). Population dynamics of the cactus Mammillaria gaumeri:
711 An integral projection model approach. *Population Ecology*, *54*(2), 321–334.
712 https://doi.org/10.1007/s10144-012-0308-7

713 Fick, S. E., & Hijmans, R. J. (2017). WorldClim 2: new 1-km spatial resolution climate surfaces
714 for global land areas. *International Journal of Climatology*, *37*(12), 4302–4315.
715 https://doi.org/10.1002/joc.5086

716 Füssel, H. M., Kristensen, P., Jol, A., Marx, A., & Hildén, M. (2017). Climate change, impacts
717 and vulnerability in Europe 2016. *An Indicator-Based Report. Luxembourg: Publications*
718 *Office of the European Union*.

719 Galiano, L., Martínez-Vilalta, J., & Lloret, F. (2010). Drought-Induced Multifactor Decline of

Scots Pine in the Pyrenees and Potential Vegetation Change by the Expansion of Co-occurring Oak Species. *Ecosystems*, *13*(7), 978–991. https://doi.org/10.1007/s10021-010-9368-8

Galiano, L., Martínez-Vilalta, J., & Lloret, F. (2011). Carbon reserves and canopy defoliation determine the recovery of Scots pine 4yr after a drought episode. *New Phytologist*, *190*(3), 750–759. https://doi.org/10.1111/j.1469-8137.2010.03628.x

Galiano, Lucía, Martínez-Vilalta, J., Eugenio, M., Granzow-de la Cerda, Í., & Lloret, F. (2013). Seedling emergence and growth of Quercus spp. following severe drought effects on a Pinus sylvestris canopy. *Journal of Vegetation Science*, *24*(3), 580–588. https://doi.org/10.1111/j.1654-1103.2012.01485.x

Guisan, A., & Thuiller, W. (2005). Predicting species distribution: Offering more than simple habitat models. *Ecology Letters*, *8*(9), 993–1009. https://doi.org/10.1111/j.1461-0248.2005.00792.x

Guisan, A., Thuiller, W., & Zimmermann, N. E. (2017). *Habitat suitability and distribution models: with applications in R*. Cambridge University Press.

Hanley, A. J., & McNeil, J. B. (1982). The Meaning and Use of the Area under a Receiver Operating Characteristic (ROC) Curve. *Radiology*, *143*, 29–36. https://doi.org/10.1148/radiology.143.1.7063747

Harris, R. M. B., Beaumont, L. J., Vance, T. R., Tozer, C. R., Remenyi, T. A., Perkins-Kirkpatrick, S. E., … Bowman, D. M. J. S. (2018). Biological responses to the press and pulse of climate trends and extreme events. *Nature Climate Change*, *8*(7), 579–587. https://doi.org/10.1038/s41558-018-0187-9

Hereş, A. M., Martínez-Vilalta, J., & López, B. C. (2012). Growth patterns in relation to drought-induced mortality at two Scots pine (Pinus sylvestris L.) sites in NE Iberian Peninsula. *Trees - Structure and Function*. https://doi.org/10.1007/s00468-011-0628-9

Jackman, S., Tahk, A., Zeileis, A., Maimone, C., Fearon, J., & Meers, Z. (2020). pscl: Classes and Methods for R Developed in the Political Science Computational Laboratory, Stanford University. *Cran*. Retrieved from https://cran.r-project.org/web/packages/pscl/pscl.pdf

Jaime, L., Batllori, E., Margalef-Marrase, J., Pérez Navarro, M. Á., & Lloret, F. (2019). Scots pine (Pinus sylvestris L.) mortality is explained by the climatic suitability of both host tree and bark beetle populations. *Forest Ecology and Management*, *448*(June), 119–129. https://doi.org/10.1016/j.foreco.2019.05.070

Jaime, L., Hart, S. J., Lloret, F., Veblen, T. T., Andrus, R., Rodman, K., & Batllori, E. (2021). Species Climatic Suitability Explains Insect–Host Dynamics in the Southern Rocky Mountains, USA. *Ecosystems*. https://doi.org/10.1007/s10021-021-00643-7

Jump, A. S., Ruiz-Benito, P., Greenwood, S., Allen, C. D., Kitzberger, T., Fensham, R., … Lloret, F. (2017). Structural overshoot of tree growth with climate variability and the global spectrum of drought-induced forest dieback. *Global Change Biology*, *23*(9), 3742–3757. https://doi.org/10.1111/gcb.13636

Karger, D. N., Conrad, O., Böhner, J., Kawohl, T., Kreft, H., Soria-Auza, R. W., … Kessler, M. (2017). Climatologies at high resolution for the earth's land surface areas. *Scientific Data*, *4*, 1–20. https://doi.org/10.1038/sdata.2017.122

Klockow, P. A., Vogel, J. G., Edgar, C. B., & Moore, G. W. (2018). Lagged mortality among tree species four years after an exceptional drought in east Texas. *Ecosphere*, *9*(10). https://doi.org/10.1002/ecs2.2455

Kuhn, M., & others. (2008). Building predictive models in R using the caret package. *Journal of Statistical Software*, *28*(5), 1–26.

Lloret, F., Keeling, E. G., & Sala, A. (2011). Components of tree resilience: Effects of successive low-growth episodes in old ponderosa pine forests. *Oikos*, *120*(12), 1909–1920. https://doi.org/10.1111/j.1600-0706.2011.19372.x

770 Lloret, F., & Kitzberger, T. (2018). Historical and event-based bioclimatic suitability predicts
771 regional forest vulnerability to compound effects of severe drought and bark beetle
772 infestation. *Global Change Biology*, (August 2017), 1952–1964.
773 https://doi.org/10.1111/gcb.14039

774 Macek, M., Wild, J., Kopecký, M., Červenka, J., Svoboda, M., Zenáhlíková, J., … Fischer, A.
775 (2017). Life and death of Picea abies after bark-beetle outbreak: Ecological processes
776 driving seedling recruitment: Ecological. *Ecological Applications*, *27*(1), 156–167.
777 https://doi.org/10.1002/eap.1429

778 Margalef-Marrase, J., Bagaria, G., & Lloret, F. (2022). Canopy Self-Replacement in Pinus
779 Sylvestris Rear-Edge Populations after Drought-Induced Die-Off. *SSRN Electronic*
780 *Journal*. https://doi.org/10.2139/ssrn.4002906

781 Margalef-Marrase, J., Pérez-Navarro, M. Á., & Lloret, F. (2020). Relationship between
782 heatwave-induced forest die-off and climatic suitability in multiple tree species. *Global*
783 *Change Biology*, *26*(5), 3134–3146. https://doi.org/10.1111/gcb.15042

784 Marquaridt, D. W. (1970). Generalized inverses, ridge regression, biased linear estimation, and
785 nonlinear estimation. *Technometrics*, *12*(3), 591–612.

786 Martínez-Vilalta, J., & Lloret, F. (2016). Drought-induced vegetation shifts in terrestrial
787 ecosystems: The key role of regeneration dynamics. *Global and Planetary Change*, *144*,
788 94–108. https://doi.org/10.1016/j.gloplacha.2016.07.009

789 Matías, L., & Jump, A. S. (2012). Interactions between growth, demography and biotic
790 interactions in determining species range limits in a warming world: The case of Pinus
791 sylvestris. *Forest Ecology and Management*, *282*, 10–22.
792 https://doi.org/10.1016/j.foreco.2012.06.053

793 Mauri, A., Strona, G., & San-Miguel-Ayanz, J. (2017). EU-Forest, a high-resolution tree
794 occurrence dataset for Europe. *Scientific Data*, *4*, 1–8.

https://doi.org/10.1038/sdata.2016.123

McDowell, N., Allen, C. D., Anderson-Teixeira, K., Brando, P., Brienen, R., Chambers, J., … Xu, X. (2018). Drivers and mechanisms of tree mortality in moist tropical forests. *New Phytologist*, *219*(3), 851–869. https://doi.org/10.1111/nph.15027

McDowell, Nate G., Allen, C. D., Anderson-Teixeira, K., Aukema, B. H., Bond-Lamberty, B., Chini, L., … Xu, C. (2020). Pervasive shifts in forest dynamics in a changing world. *Science*, *368*(6494). https://doi.org/10.1126/science.aaz9463

McDowell, Nathan G., & Allen, C. D. (2015). Darcy's law predicts widespread forest mortality under climate warming. *Nature Climate Change*, *5*(7), 669–672. https://doi.org/10.1038/nclimate2641

Mellert, K. H., Ewald, J., Hornstein, D., Dorado-Liñán, I., Jantsch, M., Taeger, S., … Kölling, C. (2016). Climatic marginality: a new metric for the susceptibility of tree species to warming exemplified by Fagus sylvatica (L.) and Ellenberg's quotient. *European Journal of Forest Research*, *135*(1), 137–152. https://doi.org/10.1007/s10342-015-0924-9

Merow, C., Dahlgren, J. P., Metcalf, C. J. E., Childs, D. Z., Margaret, E. K., Jongejans, E., … Mcmahon, S. M. (2014). Advancing population ecology with integral projection models : a practical guide, 99–110. https://doi.org/10.1111/2041-210X.12146

Metcalf, C. J. E., McMahon, S. M., Salguero-Gómez, R., & Jongejans, E. (2013). IPMpack: An R package for integral projection models. *Methods in Ecology and Evolution*, *4*(2), 195–200. https://doi.org/10.1111/2041-210x.12001

Molowny-Horas, R., Suarez, M. L., & Lloret, F. (2017). Changes in the natural dynamics of Nothofagus dombeyi forests: Population modeling with increasing drought frequencies. *Ecosphere*, *8*(3). https://doi.org/10.1002/ecs2.1708

Nambiar, E. K. S., & Sands, R. (1993). Competition for water and nutrients in forests. *Canadian Journal of Forest Research*, *23*(10), 1955–1968.

Neumann, M., Mues, V., Moreno, A., Hasenauer, H., & Seidl, R. (2017). Climate variability drives recent tree mortality in Europe. *Global Change Biology*, *23*(11), 4788–4797. https://doi.org/10.1111/gcb.13724

Niinemets, Ü., & Valladares, F. (2006). Tolerance to shade, drought, and waterlogging of temperate northern hemisphere trees and shrubs. *Ecological Monographs*, *76*(4), 521–547. https://doi.org/10.1890/0012-9615(2006)076[0521:TTSDAW]2.0.CO;2

Oliver, C. D., Larson, B. C., & others. (1996). *Forest stand dynamics*. John Wiley and sons.

Olmedo-Cobo, J. A., Gómez-Zotano, J., & Serrano-Montes, J. L. (2017). Pinus sylvestris L. subsp. nevadensis (Christ) Heywood in southern Spain: An endangered endemic Mediterranean forest. *Geographica Pannonica*, *21*(3), 151–165. https://doi.org/10.5937/GeoPan1703151O

Peltola, H., Kilpeläinen, A., & Kellomäki, S. (2002). Diameter growth of Scots pine (Pinus sylvestris) trees grown at elevated temperature and carbon dioxide concentration under boreal conditions. *Tree Physiology*, *22*(14), 963–972. https://doi.org/10.1093/treephys/22.14.963

Pérez Navarro, M. Á., Sapes, G., Batllori, E., Serra-Diaz, J. M., Esteve, M. A., & Lloret, F. (2018). Climatic Suitability Derived from Species Distribution Models Captures Community Responses to an Extreme Drought Episode. *Ecosystems*, *22*(1), 77–90. https://doi.org/10.1007/s10021-018-0254-0

Pimm, S. L. (1984). The complexity and stability of ecosystems. *Nature*, *307*(5949), 321–326. https://doi.org/10.1038/307321a0

Press, W. H., Flannery, B. P., Teukolsky, S. A., & Vetterling, W. T. (1989). *Numerical recipes. The art of scientific computing*. Cambridge, England: Cambridge University Press.

Ramula, S., Rees, M., & Buckley, Y. M. (2009). Integral projection models perform better for small demographic data sets than matrix population models: A case study of two perennial

herbs. *Journal of Applied Ecology*, *46*(5), 1048–1053. https://doi.org/10.1111/j.1365-2664.2009.01706.x

Redmond, M. D., Weisberg, P. J., Cobb, N. S., & Clifford, M. J. (2018). Woodland resilience to regional drought: Dominant controls on tree regeneration following overstorey mortality. *Journal of Ecology*, *106*(2), 625–639. https://doi.org/10.1111/1365-2745.12880

Ridgeway, G. (2007). Generalized Boosted Models: A guide to the gbm package. *Compute*, *1*(4), 1–12. https://doi.org/10.1111/j.1467-9752.1996.tb00390.x

Rigby, R. A., & Stasinopoulos, D. M. (2005). Generalized additive models for location , scale, 507–554.

Ruiz-Benito, P., Lines, E. R., Gómez-Aparicio, L., Zavala, M. A., & Coomes, D. A. (2013). Patterns and Drivers of Tree Mortality in Iberian Forests: Climatic Effects Are Modified by Competition. *PLoS ONE*, *8*(2). https://doi.org/10.1371/journal.pone.0056843

Sánchez-Salguero, R., Navarro-Cerrillo, R. M., Swetnam, T. W., & Zavala, M. A. (2012). Is drought the main decline factor at the rear edge of Europe? The case of southern Iberian pine plantations. *Forest Ecology and Management*, *271*, 158–169. https://doi.org/10.1016/j.foreco.2012.01.040

Sánchez-Velásquez, L. R., Pineda-López, M. del R., Ibarra-Zavaleta, S. P., & López-Serrano, Y. (2021). Fir forest demography using matrix projections: Anomaly precipitation due to climatic change decrease population viability. *Forest Ecology and Management*, *482*(December 2020). https://doi.org/10.1016/j.foreco.2020.118845

Sanderson, B. M., Knutti, R., & Caldwell, P. (2015). A representative democracy to reduce interdependency in a multimodel ensemble. *Journal of Climate*, *28*(13), 5171–5194. https://doi.org/10.1175/JCLI-D-14-00362.1

Sapes, G., Serra-Diaz, J. M., & Lloret, F. (2017). Species climatic niche explains drought-induced die-off in a Mediterranean woody community. *Ecosphere*, *8*(5).

https://doi.org/10.1002/ecs2.1833

Senf, C., Buras, A., Zang, C. S., Rammig, A., & Seidl, R. (2020). Excess forest mortality is consistently linked to drought across Europe. *Nature Communications*, *11*(1), 1–8. https://doi.org/10.1038/s41467-020-19924-1

Serra-Maluquer, X., Mencuccini, M., & Martínez-Vilalta, J. (2018). Changes in tree resistance, recovery and resilience across three successive extreme droughts in the northeast Iberian Peninsula. *Oecologia*, *187*(1), 343–354. https://doi.org/10.1007/s00442-018-4118-2

Sohn, J. A., Hartig, F., Kohler, M., Huss, J., & Bauhus, J. (2016). Heavy and frequent thinning promotes drought adaptation in Pinus sylvestris forests. *Ecological Applications*, *26*(7), 2190–2205. https://doi.org/10.1002/eap.1373

Stasinopoulos, D. M., & Rigby, R. A. (2007). Generalized additive models for location scale and shape (GAMLSS) in R. *Journal of Statistical Software*, *23*(7), 1–46. https://doi.org/10.18637/jss.v023.i07

Suarez, M. L., & Lloret, F. (2018). Self-replacement after small-scale partial crown dieback in austral Nothofagus dombeyi forests affected by an extreme drought. *Canadian Journal of Forest Research*, *48*(4), 412–420. https://doi.org/10.1139/cjfr-2017-0305

Vilà-Cabrera, A., Martínez-Vilalta, J., Galiano, L., & Retana, J. (2013). Patterns of Forest Decline and Regeneration Across Scots Pine Populations. *Ecosystems*, *16*(2), 323–335. https://doi.org/10.1007/s10021-012-9615-2

Wong, C. M., & Daniels, L. D. (2017). Novel forest decline triggered by multiple interactions among climate, an introduced pathogen and bark beetles. *Global Change Biology*, *23*(5), 1926–1941. https://doi.org/10.1111/gcb.13554

Tables

Table 1: Generalized linear model with binominal distribution and GAMLSS terms for survival and growth, respectively, at the plot level. Dependent variables were: plot basal area (BA plot, $m^2\ ha^{-1}$), dbh at t_0), tree density (N, number of trees · ha^{-1}), climatic suitability (CS) and die-off effect (yes/no).

Function	*Family Model*		*Intercept*	*BA plot*	*dbht$_0$*	*dbht$_0^2$*	*N*	*CS*	*Die-off [Yes]*
Survival	**Binomial**		3.335	-0.961	0.080	-0.001	-	-	-
Growth	**GAMLSS**	***Mu coeff.***	-2.122	-0.506	0.022	$-2.00 \cdot 10^{-4}$	-0.007	2.901	-
		Sigma coeff.	-0.274	0.157	-0.004	-	-	-	-0.120

Table 2: Zero-inflated regression models terms (columns) for total number of seedlings, saplings and ingrowth at time (t_1). Variables represented in rows aren1$_{t0}$: Number of seedlings at t_0 (number of seedlings · ha^{-1}), $n2_{t0}$: number of saplings at time t_0 (number of saplings · ha^{-1}). Other environmental variables used were basal area ($m^2\ ha^{-1}$), climatic suitability and die-off effect (yes/no).

	n. of seedlings t_1	***n. saplings t_1***	***n. Ingrowth t_1***
Count component			
Intercept	-5.4804	1.3143	-3.7629
Basal Area	-2.727	-0.3831	-9.6048
(Basal Area)$^{0.5}$	4.7794	-	12.0489
$n1_{t0}$	0.0173	0.0105	-
$n2_{t0}$	-	0.0537	0.1234
Climatic Suitability	7.1219	-	-
Die-off [Yes]	-1.0247	-	-
Zero component			
Intercept	-0.6138	2.5618	3.895
$n2_{t0}^{0.5}$	-	-2.8698	-3.295

Table 3: Results of the GLMMs built to assess the factors determining stand dynamics over time, for the following response variables: basal area, seedling density, ingrowth density, sapling density, mean diameter and tree density for the whole period. GLMMs considered time since the die-off event – year (time) –, die-off effect [yes *vs* no] and climate change scenarios – abbreviated as CCscenario – [RCP4.5, RCP8.0 vs. current constant climate] as explanatory factors. The estimates and significance (*p* value) of the factors for the response variables are represented in rows. Interactions between factors are also included. The variances explained by the fixed effects of the models – r^2m– are represented in the last row.

	Basal area		**Seedling density**		**Ingrowth density**	
	Estimate	*p*	Estimate	*p*	Estimate	*p*
Intercept	-0.083	<0.0001	3.749	<0.0001	-0.522	<0.0001
Die-off [Yes]	-0.598	0.0020	1.168	<0.0001	1.698	<0.0001
CCscenario[RCP4.5]	-2.819	<0.0001	-0.429	<0.0001	0.422	<0.0001
CCscenario[RCP8.0]	-2.670	<0.0001	-0.393	<0.0001	0.398	<0.0001
Die-off [Yes]:RCP45	0.207	0.5940	-0.307	<0.0001	-0.198	0.104
Die-off [Yes]:RCP80	0.219	0.5738	-0.285	<0.0001	-0.189	0.122
Year (time)	0.430	<0.0001	-0.071	<0.0001	-0.047	<0.0001
Die-off [Yes]:Year	0.019	0.0426	0.021	<0.0001	0.121	<0.0001
r^2m	*0.51*		*0.49*		*0.329*	

	Sapling density		***Mean Diameter***		***Tree Density***	
	Estimate	*p*	*Estimate*	*p*	*Estimate*	*p*
Intercept	-2.834	<0.0001	2.860	<0.0001	6.759	<0.0001
Die-off [Yes]	0.054	<0.0001	-8.631	0.179	-8.805	<0.0001
CCscenario[RCP4.5]	0.034	0.466	-2.964	0.0002	0.004	0.770
CCscenario[RCP8.0]	0.032	0.494	-2.889	0.0003	0.005	0.750
Die-off [Yes]:RCP45	-0.075	0.258	-0.191	0.109	-0.198	0.104
Die-off [Yes]:RCP80	-0.071	0.283	-0.160	0.151	-0.189	0.122
Year (time)	0.101	<0.0001	0.571	<0.0001	-0.015	<0.0001
Die-off [Yes]:Year	0.008	0.260	0.023	<0.0001	0.057	<0.0001
r^2m	*0.41*		*0.16*		*0.14*	

Table 4: Results of the GLMMs built to assess the factors determining the following response variables at the final of the projected period (year 2069):basal area, seedling density, ingrowth density, sapling density, mean diameter and tree density. The GLMMs considereddie-off effects [yes *vs* no] and climate change scenarios – abbreviated as CCscenario – [RCP4.5, RCP8.0 vs. current constant climate CCscenario] as explanatory factors. The estimates and significance (*p* value) of the factors for the response variables are represented in rows. Interactions between factors are also included. The variances explained by the fixed effects of the models – r^2m– are represented in the last row.

	Basal area		***Seedling density***		***Sapling density***	
	Estimate	*p*	*Estimate*	*p*	*Estimate*	*p*
Intercept	4.095	<0.0001	2.660	<0.0001	47.628	<0.0001
Die-off[yes]	-0.477	0.0002	1.249	<0.0001	43.224	<0.0001
CCscenario[RCP4.5]	-0.123	<0.0001	-0.619	<0.0001	5.675	<0.0001
CCscenario [RCP8.0]	-0.112	<0.0001	-0.487	<0.0001	5.438	<0.0001
Die-off[Yes]:RCP4.5	-0.081	0.024	-0.391	0.0116	-7.935	<0.0001
Die-off[Yes]:RCP8.0	-0.076	0.034	-0.361	0.0194	-7.317	<0.0001
r^2m	*0.30*		*0.53*		*0.47*	

Table 4 extended:

	Ingrowth density		***Mean diameter***		***Tree density***	
	Estimate	*p*	*Estimate*	*p*	*Estimate*	*p*
Intercept	-2.331	<0.0001	3.458	<0.0001	6.521	<0.0001
Die-off[yes]	3.297	<0.0001	-0.285	0.0084	-0.091	0.0084
CCscenario[RCP4.5]	1.178	<0.0001	-0.075	<0.0001	5.675	<0.0001
CCscenario[RCP8.0]	1.095	<0.0001	-0.069	<0.0001	5.438	<0.0001
Die-off[Yes]:RCP4.5	-0.391	0.0538	-0.057	0.0150	-7.935	<0.0001
Die-off[Yes]:RCP8.0	-0.362	0.0734	-0.052	0.0251	-7.317	<0.0001
r^2m	0.40		0.19		0.10	

Figures

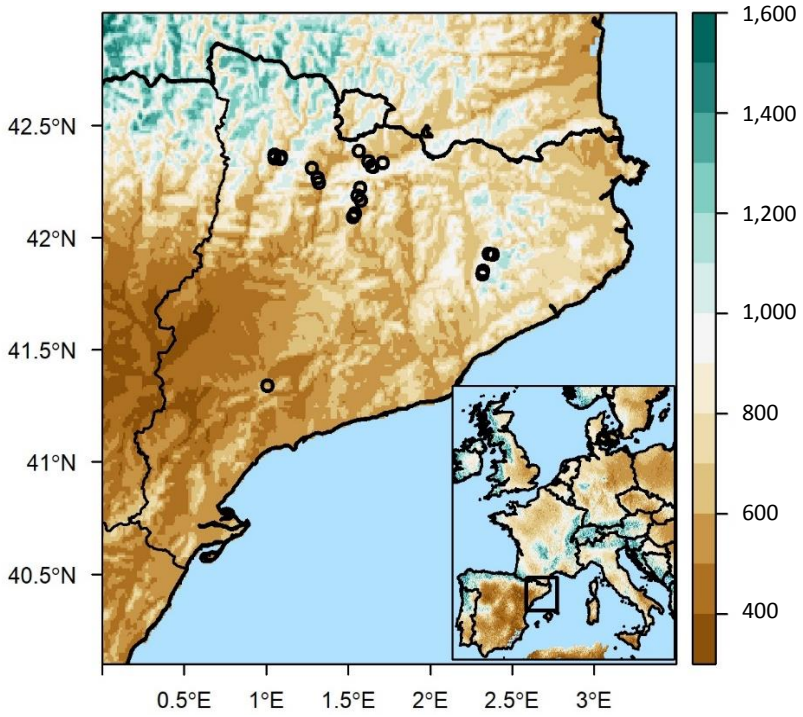

Figure 1: Mean annual precipitation (mm) in our study area. Map generated with data extracted from: CHELSA climate database (Karger et al., 2017). The location of the 20 sampled *P. sylvestris* populations are represented as blackcircles.

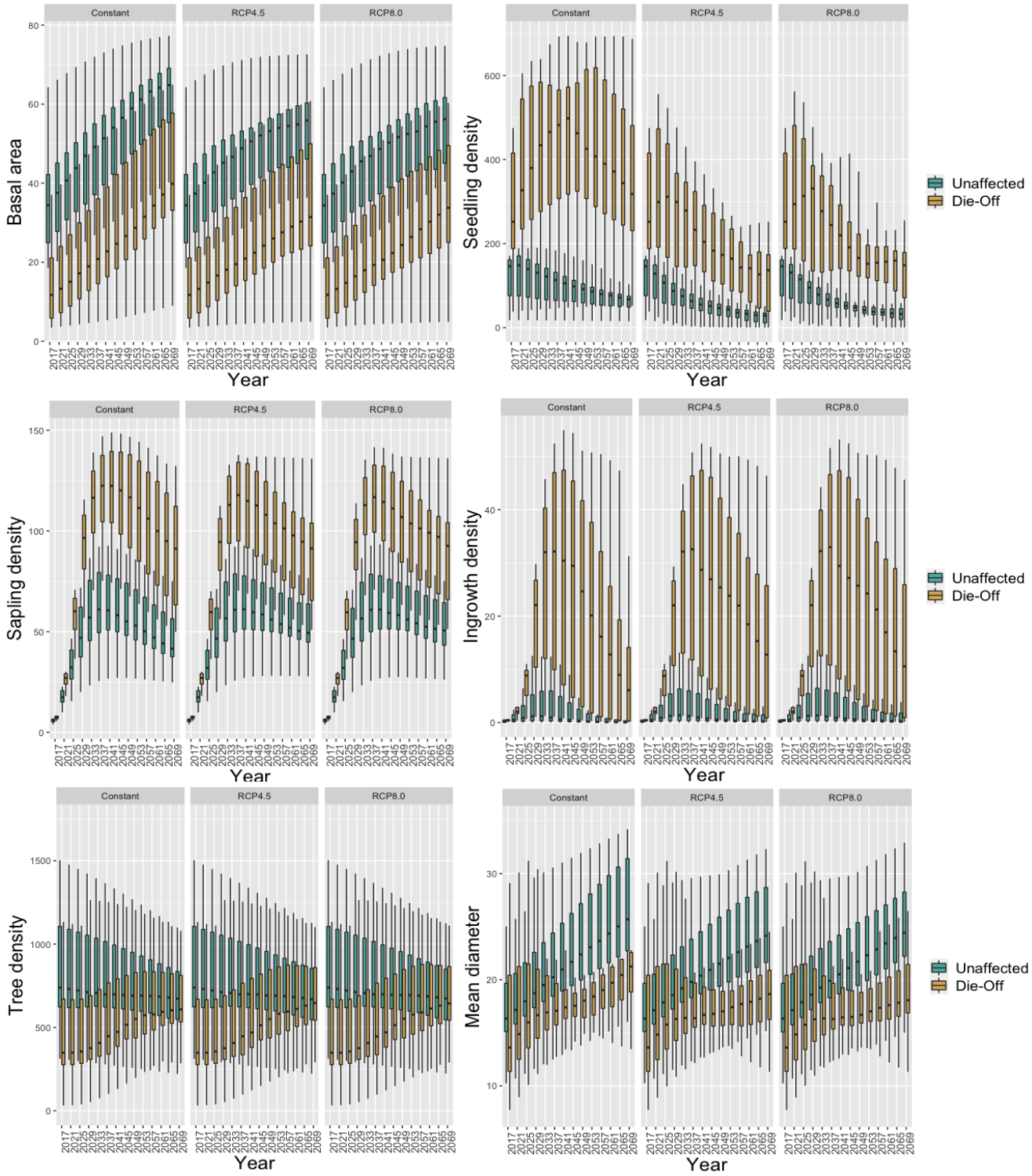

Figure 2: Structural and demographic variables of the plots extracted from IPM outputs: basal area, seedling density, sapling density, ingrowth density, tree density (adult tree density), mean diameter, for plots with die-off and for unaffected ones, under different climatic scenarios (Constant, current climate *vs*. RCP4.5 and RCP8.0). Represented as boxplots. Boxes indicate the interquantile range of the response variables obtained in the simulations; black lines indicat standard deviation above and below the mean.

Declaration of Interest Statement

The authors declare that they have no known competing financial interests or personal relationships that could have appeared to influence the work reported in this paper.

Author Contributions Statement

F. Lloret, J. Margalef-Marrase and R. Molowny-Horas conceived the ideas and designed the methodology; L. Jaime and J. Margalef-Marrase collected field data; R. Molowny-Horas and J. Margalef-Marrase analyzed the data; J. Margalef-Marrase led the writing of the manuscript. All authors contributed critically to the drafts and gave final approval for publication.